JOURNAL OF AIRCRAFT
Vol. 37, No. 2, March–April 2000

Engineering Notes

ENGINEERING NOTES are short manuscripts describing new developments or important results of a preliminary nature. These Notes cannot exceed 6 manuscript pages and 3 figures; a page of text may be substituted for a figure and vice versa. After informal review by the editors, they may be published within a few months of the date of receipt. Style requirements are the same as for regular contributions (see inside back cover).

Lift Augmentation for Massive Separation

W. W. H. Yeung*
Nanyang Technological University, Singapore 639798, Republic of Singapore

Introduction

THE increasing demand for additional lift and high wing loads for vertical and short takeoff and landing aircraft leads to continual research on lift enhancement both theoretically and experimentally. Earlier powered high-lift systems[1] include slotted and externally blown flaps, boundary-layer control, and augmentor-wing concept. The high lift-drag ratios of the Kasper wing at low speeds motivated the theoretical studies[2] of additional lift induced on airfoils by a standing vortex. The concept of spanwise fences[3] on an airfoil was introduced to trap a stationary vortex for lift enhancement. Another means of utilizing a vortex to enhance lift was to incorporate a backward-facing step.[4] Recently, wind-tunnel tests[5] showed that a vortex plate located on the upper surface of a blunt-edged delta wing is capable of increasing lift.

The present theoretical study was motivated by the flow visualization picture[6] of flow around a flat plate experiencing leading-edge stall at an angle of attack $\alpha = 2.5$ deg at which the flow was characterized by separation at the leading edge and followed by downstream reattachment to form a separation bubble. In Fig. 1a the pressure distribution on a flat plate with leading-edge stall[7] at $\alpha = 5.85$ deg is compared with the prediction from the Kutta–Joukowsky model of attached flow,

$$C_P = 1 - \frac{[\sin(\phi - \alpha) + \sin\alpha]^2}{\sin^2\phi} \tag{1}$$

where $2x/c = 1 + \cos\phi$. The theoretical distribution over $0 \le x/c \le 0.5$ on the upper surface is strongly influenced by the presence of the separation bubble. However, Fig. 1b shows that lift predicted by the Kutta–Jouskowsky model

$$C_L = 2\pi \sin\alpha \tag{2}$$

agrees well with the measurements[7] for leading-edge stall ($0 < \alpha \le 9$ deg). As α is increased to 15 deg, the flow visualization picture[8] reveals that the leading-edge separation spreads rearward and reattachment on the upper surface of the plate is no longer possible. The experimental pressure distribution associated with such massive separated flow[7] at $\alpha = 14.85$ deg is completely different from the prediction of Eq. (1) as shown in Fig. 1b. When massive separation takes place over the upper surface at $\alpha > 9$ deg, there is a drastic loss of lift in Fig. 1c. The prediction from Eq. (3) from the Kirchhoff–Helmholtz model for separated flow is also inaccurate.

$$C_L = \frac{\pi \sin 2\alpha}{4 + \pi \sin\alpha} \tag{3}$$

Received 17 January 1999; revision received 23 November 1999; accepted for publication 24 November 1999.

*Associate Professor, School of Mechanical and Production Engineering.

Lift may be enhanced if the leading-edge separation and subsequent massive separation are avoided by adding a positive camber to the leading edge of the flat plate. A fixed camber is only applicable to a particular angle of attack. In this Note, instead of avoiding separation, the idea of using it and its subsequent reattachment to provide additional lift is explored. The resulting shear layer emanating from the leading edge and terminating on reattachment divides the internal recirculating flow from the external flow. In the context of potential flow, it behaves like a solid boundary and thus adds a positive camber to the flat plate. Flow over the boundary will be more likely attached because it can negotiate on the streamlined surface. A portion of this boundary is preferably not fixed in shape such that it can be adjusted to accommodate the variation of angle of attack. The flexibility in camber will be manipulated by using flow-control elements located inside the recirculating zone. To prevent the shear layer from breaking up caused by instability, its length should not be too long. Therefore, the rear portion of the shear layer is best replaced by a forward-facing fence, which joins the upper surface of the flat plate tangentially.

A similar model of free-streamline theory was proposed[9] to exploit the boundary-layer control to reattach the separated flow to the upper surface of a forward-facing flap located above a wing. Instead of using the hodograph method, the present model in the physical plane is conformally mapped to and solved in a complex plane such that the leading and trailing edges of the airfoil and the tip of the fence are critical points in the mapping sequence. In addition, a curved fence, whose curvature follows from the mapping, replaces the straight fence such that the flow is streamlined. The stagnation points at the bases of the spanwise fence[3] are eliminated because they tend to reduce the lift and increase the drag substantially. Besides, the condition of a streamline having finite curvature or pressure gradient is satisfied at reattachment, where necessary. The model has been shown for enhancing lift in the presence of thin airfoil stall.[10] Predictions are compared other theoretical and experimental results to demonstrate its feasibility.

Mathematical Formulation

Consider incompressible inviscid uniform flow U as an angle of attack α approaches the flat plate of unit chord in plane $Z = x + iy$, with the leading and trailing edges at $x = 0$ and c. The following conformal transformations

$$Z = A(Z_1 + 1/Z_1) + B, \qquad Z_1 = (1 + i/Z_2)\exp(i\theta_0)$$
$$CZ_2 - 2\pi/h + 1 = Z_3 - \log Z_3, \qquad \zeta = G(D + Z_3)/(E - Z_3) \tag{4}$$

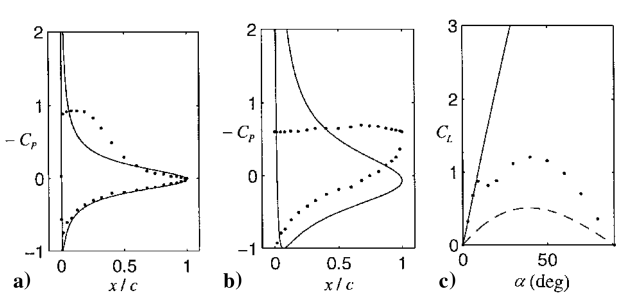

Fig. 1 Comparison of pressure distributions and lift variations: a) $\alpha = 5.85$ deg; b) $\alpha = 14.85$ deg; c) – – –, Kirchhoff–Helmholtz; ——, Kutta–Joukowsky; and ●, experiment.[7]

map the flat plate to a unit circle $\zeta = \exp(i\theta)$ centered at the origin of the ζ plane. A, B, C, D, E, and G are constants for scaling and translation. The straight forward-facing fence SB in the auxiliary plane Z_1 has a length h. SB is, however, a curved segment in the Z plane and intersects the plate tangentially at B, which is located at $X_B = (1 + \cos\theta_0)/2$ measured from the leading edge. It is readily shown from Eq. (4) that $dZ/d\zeta = 0$ at L (leading edge), T (trailing edge), and S (tip of fence).

The complex velocity $W(Z)$ is related to the complex potential $F(\zeta)$ by

$$W(Z) = \frac{dF}{d\zeta}\frac{d\zeta}{dZ} \tag{5}$$

By Bernoulli's equation the pressure distribution on the bounding streamline, plate, and fence is given by

$$C_P = 1 - |W(Z)/U|^2 \tag{6}$$

The basic flow elements in the ζ plane consist of the uniform flow V, a doublet of strength V, and a vortex of strength Γ both at the origin. The latter provides finite velocity at the trailing edge at any value of α. Therefore, the complex potential is

$$F_b(\zeta) = V(\zeta + 1/\zeta) + (i\Gamma/2\pi)\ln\zeta \tag{7}$$

The bounding streamline joining the leading edge and the tip of the fence imposes the condition that the additional flow elements have zero net flow. Three simple models are proposed as follows:

1) Doublet model:

$$F(\zeta) = F_b(\zeta) - (Q_0/2\pi)\exp(i\delta)/[\zeta - \exp(i\delta)] \tag{8}$$

where Q_D is the strength of a doublet tangential to the unit circle at $\zeta = \exp(i\delta)$. Γ, Q_D, and δ can be determined by satisfying $dF/d\zeta = 0$ at L, T, and S.

2) Source/sink model:

$$F(\zeta) = F_b(\zeta) + (Q/2\pi)\ln\{[\zeta - \exp(i\delta_1)]/[\zeta - \exp(i\delta_2)]\} \tag{9}$$

Γ, Q, δ_1, and δ_2 are uniquely determined by satisfying $dF/d\zeta = 0$ at L, T, and S, and an additional condition at S. The source and the sink will combine to form a doublet when $\delta_1 \to \delta_2$, and it occurs as h is increased at a fixed value of X_B.

3) Three-vortex model:

$$F(\zeta) = F_b(\zeta) + (i\Gamma_1/2\pi)\ln\{[\zeta - R\exp(i\delta)]/[\zeta - R^{-1}\exp(i\delta)]\} \tag{10}$$

Similar to the source/sink model, Γ, Γ_1, R, and δ are determined by satisfying $dF/d\zeta = 0$ at L, T, and S, and an additional condition at S. When h is decreased at a given value of X_B, $R \to 1$, and three-vortex model will become the doublet model.

The vortex in the physical plane in some previously mentioned theoretical studies[2,3] is stationary. The presently proposed flow models involve a doublet, source and sink or vortices so that the condition of stationary vortex is not necessarily applicable. By differentiating Eq. (1), it can be shown that the pressure gradient at the trailing edge of the flat plate is infinite because the separation streamline has a curvature different from that of the plate. A class of airfoils[11] having finite trailing-edge pressure gradients was developed. As indicated in the model for airfoils experiencing trailing-edge stall,[12] this condition provides predictions of pressure in reasonable agreement with wind-tunnel data. Because the pressure gradient at the leading edge of the plate is generally steep and is infinite at the trailing edge, this condition is more reasonable at reattachment. The condition of finite pressure gradient at point S is

$$f_1'' f_2' - f_2'' f_1' = 0 \tag{11}$$

where $f_1 = |dF/d\zeta|$, $f_2 = |dZ/d\zeta|$, and the derivative $(\,)'$ is taken with respect to θ.

Results

For the doublet model the shapes of the bounding streamline, fence, flat plate, and location of doublet are shown in the physical plane in Fig. 2a for $\alpha = 14.85$ deg, $h = 0.7$, and $X_B = 0.5$. As shown,

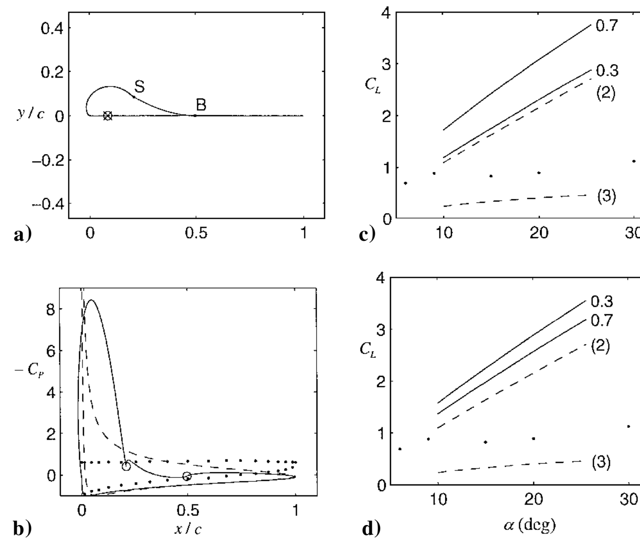

Fig. 2 Doublet model at $\alpha = 14.85$ deg (●, experiment[7]): a) Z plane, ⊗, doublet; b) ——, present; - - -, Eq. (1) at $h = 0.7$, $X_B = 0.5$; c) C_L vs α for $h = 0.7$: $X_B = 0.7, 0.3$; and d) C_L vs α for $X_B = 0.5$: $h = 0.3, 0.7$.

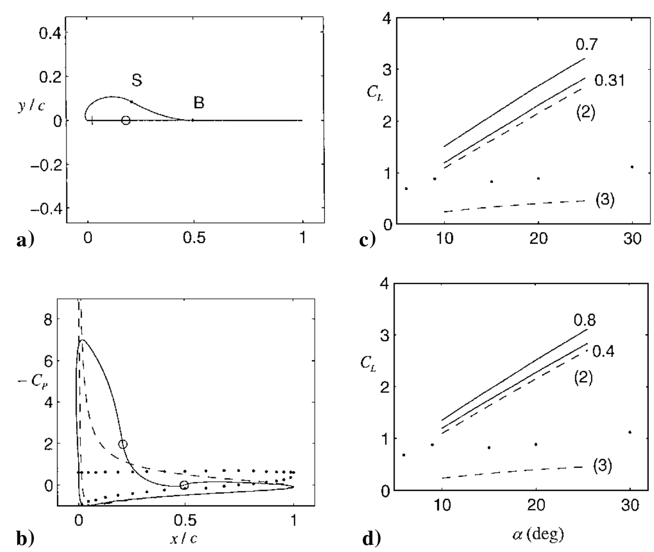

Fig. 3 Source/sink model at $\alpha = 14.85$ deg (●, experiment[7]): a) Z plane, (+, ○): source/sink; b) ——, present; - - -, Eq. (1) at $h = 0.7$, $X_B = 0.5$; c) C_L vs α for $h = 0.7$: $X_B = 0.7, 0.31$; and d) C_L vs α for $X_B = 0.5$: $h = 0.8, 0.4$.

the maximum thickness of the bounding streamline is $y/c = 0.13$ at $x/c = 0.094$, and the doublet is located at $x/c = 0.083$. The infinite and narrow suction peak at the leading edge from Eq. (1) is replaced by a finite and broader suction peak from of the present model, as shown in Fig. 2b. Although the pressure distributions on the upper surface from the two models are significantly different from each other, those on the lower surface are almost identical. At the trailing edge the present model offers $C_P = 0.105$, which is more positive than $C_P = 0.066$ from Eq. (1) and $C_P = -0.6$ from experiment.[7] When comparing with the attached flow model, an increase in lift of 21.4% is found. The pressure gradient is finite at B but infinite at S. Variations of C_L with α at different values of X_B and h are found in Figs. 2c and 2d, respectively.

Figure 3a shows the bounding streamline in the Z plane by using the source/sink model for $\alpha = 14.85$ deg, $h = 0.7$, and $X_B = 0.5$. The maximum thickness of the bubble is $y/c = 0.105$ at $x/c = 0.119$ while the source and sink are at $x/c = 0.022$ and 0.181, respectively. The pressure distribution of the present model is compared with Eq. (1) and the experimental data[7] in Fig. 3b, highlighting finite pressure gradients at points B and S. Again, the present model produces a finite suction peak at the leading edge. At the trailing

Table 1 Comparison of theoretical models and experiment at $\alpha = 14.85$ deg

$h = 0.7$, $X_B = 0.5$	min C_P	C_L	$h = 1$, $X_B = 0.5$	min C_P	C_L
Doublet	-8.43	1.955	Doublet	-8.75	1.953
Source/sink	-7.00	1.876	Three-vortex	-10.6	1.997
Eq. (2)	$-\infty$	1.610	Eq. (2)	$-\infty$	1.610
Eq. (3)	0	0.324	Eq. (3)	0	0.324
Experiment[7]	-0.69	0.883	Experiment[7]	-0.69	0.883

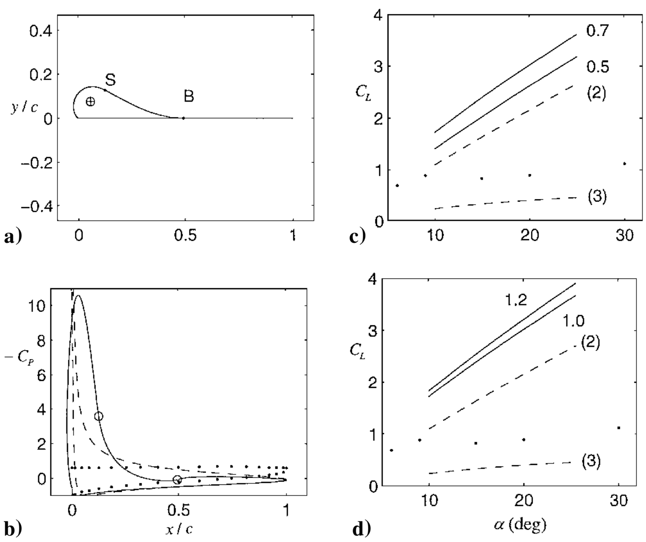

Fig. 4 Three-vortex model at $\alpha = 14.85$ deg (•, experiment[7]): a) Z plane, ⊕, vortex; b) ——, present; – – –, Eq. (1), $h = 1$, $X_B = 0.5$; c) C_L vs α for $h = 1$: $X_B = 0.7, 0.5$; and d) C_L vs α for $X_B = 0.7$: Eq. (1) $h = 1.2, 1.0$.

edge the present model offers $C_P = 0.098$, which is higher than those values from Eq. (1) and the experiment.[7] The lift coefficient is increased by 16.5%. At given values of X_B and h, C_L increases with α, as shown in Figs. 3c and 3d.

The location of the external vortex, shape of bounding streamline, fence and plate for the three-vortex model are shown in Fig. 4a at $\alpha = 14.85$ deg, $h = 1$, and $X_B = 0.5$. The bubble has $y_{max}/c = 0.144$ at $x/c = 0.067$ and trailing edge of $C_P = 0.117$, both slightly larger than $y_{max}/c = 0.1311$ at $x/c = 0.092$ and $C_P = 0.102$ from the doublet model under the same condition. The finite suction peak at the leading edge and finite pressure gradients at S and B are shown in Fig. 4b. In comparison with the attached flow model, C_L is increased by 24.1%. At fixed values of X_B and h, variations of C_L with α are depicted in Figs. 4c and 4d, respectively. Table 1 compares some results from the theoretical models and experimental measurements.

Conclusion

An analytical method is proposed for augmenting the lift on a flat plate experiencing massive separation on its suction side. At any positive angle of attack, the separated flow at the leading edge is made to reattach smoothly to a forward-facing fence by suitable mathematical singularities subject to available boundary conditions. A bounding streamline, which emanates from the separation point and terminates at the tip of the fence joining the plate tangentially on its upper surface to prevent any unnecessary stagnated flow, increases the camber and thickness of the plate. Finite velocity is enforced at each of the critical points of the conformal mapping, namely the tip of the fence and leading and trailing edges of the plate. In addition, the condition of finite pressure gradient at reattachment is satisfied where applicable. Numerical results from varying the length of the fence and its location with respect to the leading edge suggest that lift on the flat plate is enhanced, when compared with the predictions from the attached flow model by Kutta–Joukowsky, the separated flow theory by Kirchhoff–Helmholtz, and measurements by Fage and Johansen.

References

[1] Korbacher, G. K., "Aerodynamics of Powered High-Lift Systems," *Annual Review of Fluid Mechanics*, Vol. 6, 1974, pp. 319–358.

[2] Huang, M., and Chow, C., "Trapping of a Free Vortex by Joukowski Airfoils," *AIAA Journal*, Vol. 20, No. 3, 1982, pp. 292–298.

[3] Rossow, V. J., "Aerodynamics of Airfoils with Vortex Trapped by Two Spanwise Fences," *Journal of Aircraft*, Vol. 31, No. 1, 1994, pp. 146–153.

[4] Finaish, F., and Witherspoon, S., "Aerodynamic Performance of an Airfoil with Step-Induced Vortex for Lift Augmentation," *Journal of Aerospace Engineering*, Vol. 11, Jan. 1998, pp. 9–16.

[5] Traub, L. W., "Efficient Lift Enhancement of a Blunt Edged Delta Wing," *The Aeronautical Journal*, Nov. 1997, pp. 439–445.

[6] Werle, H., "Le Tunnel Hydrodynamique au Service de la Recherche Aerospatiale," Publication No. 156, ONERA, France, 1974, (Photograph 35 in Van Dyke, M., *An Album of Fluid Motion*, The Parabolic Press, CA, 1988).

[7] Fage, A., and Johansen, F. C., "On the Flow of Air Behind an Inclined Flat Plate of Infinite Span," *Proceedings of the Royal Society of London*, A Vol. 116, Sept. 1927, pp. 170–197.

[8] Japan Society of Mechanical Engineers, *Visualized Flow*, Pergamon, Oxford, 1988 (Photograph 130), p. 79.

[9] Hurley, D. G., "The Use of Boundary Layer Control to Establish Free Streamline Flows," *Advances in Aeronautical Science*, Vol. 2, 1959, pp. 662–708.

[10] Yeung, W. W. H., and Parkinson, G. V., "A Theoretical Investigation of Enhanced Lift in the Presence of Thin Aerofoil Stall," *The Aeronautical Journal*, May 1999, pp. 237–244.

[11] Ormsbee, A. I., and Maughmer, M. D., "A Class of Airfoils Having Finite Trailing-Edge Pressure Gradients," *Journal of Aircraft*, Vol. 23, No. 2, 1986, pp. 97–103.

[12] Yeung, W. W. H., and Parkinson, G. V., "A Wake Singularity Potential Flow Model for Airfoils Experiencing Trailing-Edge Stall," *Journal of Fluid Mechanics*, Vol. 251, June 1993, pp. 203–218.

Moving-Wall Effect on Unsteady Boundary Layers

H. Dumitrescu* and V. Cardoş†

Caius Iacob Institute of Applied Mathematics, RO 70700, Bucharest, Romania

I. Introduction

MOVING-WALL effect for airfoils refers to the unsteady wall boundary condition, which may lead to different courses of leading-edge separation. An airfoil oscillating at large angles of attack presents a well-known case of dynamic stall, characterized by a delay in the onset of boundary-layer separation. Two contributions are responsible for this overall delay: one is caused by the beneficial accelerated flow effects on the developing boundary layer during the angle of attack increasing phase, and the other is caused by the moving-wall effect illustrated in Fig. 1 (Ref. 1).

As the leading edge moves upward during the upstroke, the boundary layer is strengthened and stall delayed because of the large difference in tangential wall velocities at the flow stagnation and separation points on the upper side of the airfoil. There the boundary layer has a fuller velocity profile and is, therefore, more difficult to separate. Figure 1 clearly shows that the moving-wall effect will be different for an airfoil oscillating in a uniform stream in pitching and plunging modes. Thus, when the effective angle of attack is increasing, the moving-wall effect is favorable for the pitching airfoil, whereas it is adverse for the equivalent plunging airfoil, with the nose in downward stroke. In spite of this fact and the experimental findings,[2] most dynamic stall analysis methods[3]

Received 23 June 1999; revision received 2 July 1999; accepted for publication 21 September 1999.

*Professor and Senior Researcher, Romanian Academy, P.O. Box 1-24.

†Senior Researcher, Romanian Academy, P.O. Box 1-24.